

LITERATURE REVIEW SUPPORTING  
ASSESSMENT OF POTENTIAL RADIONUCIDES  
IN THE 291-Z EXHAUST VENTILATION

L. A. Mahoney  
M. Y. Ballinger  
W. E. Davis<sup>(a)</sup>  
S. J. Jette  
L. M. Thomas  
J. A. Glissmeyer

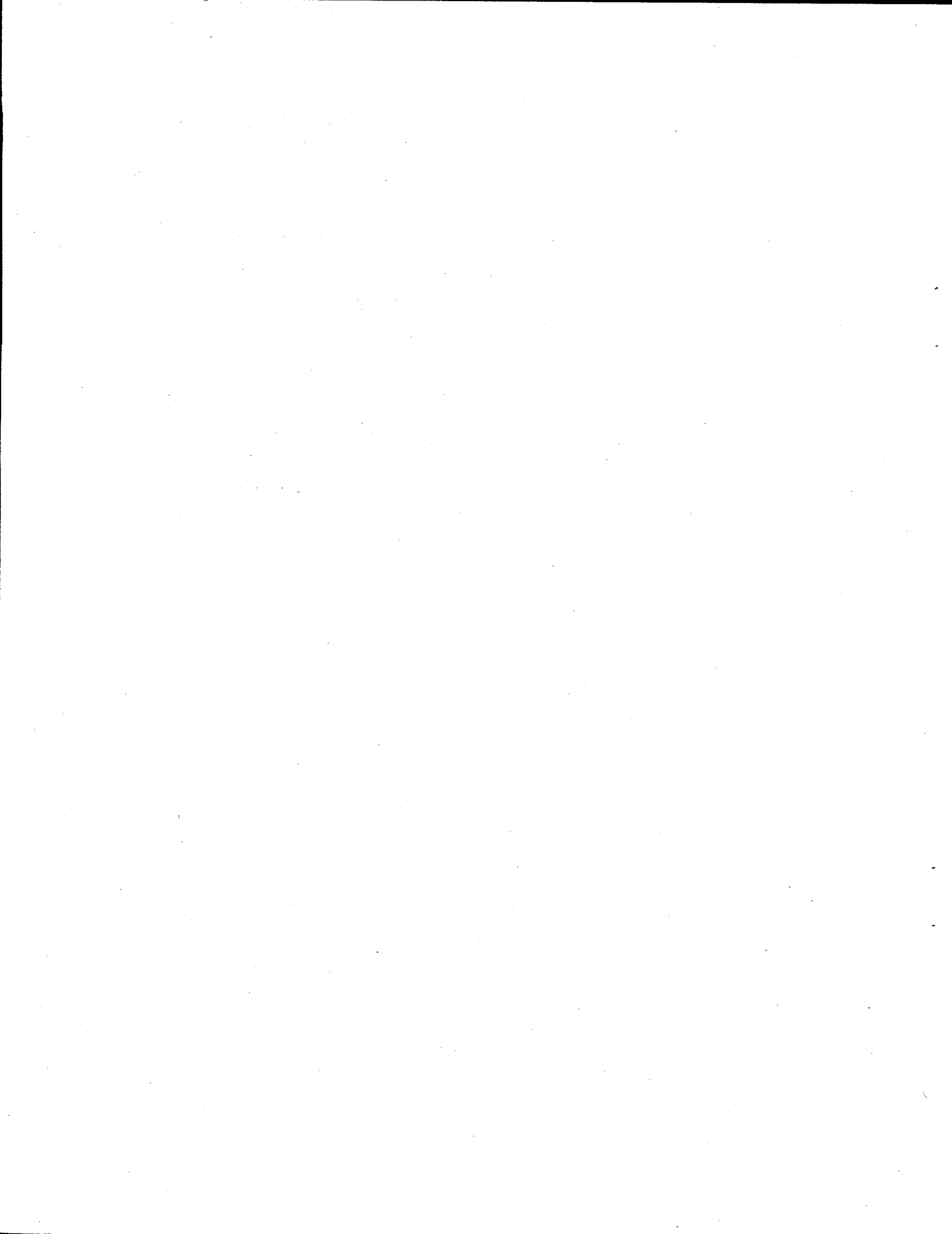
August 1994

Prepared for  
the U.S. Department of Energy  
under Contract DE-AC06-76RLO 1830

Pacific Northwest Laboratory  
Richland, Washington 99352

(a) Westinghouse Hanford Company

MASTER  
REP



## **DISCLAIMER**

**This report was prepared as an account of work sponsored by an agency of the United States Government. Neither the United States Government nor any agency thereof, nor any of their employees, make any warranty, express or implied, or assumes any legal liability or responsibility for the accuracy, completeness, or usefulness of any information, apparatus, product, or process disclosed, or represents that its use would not infringe privately owned rights. Reference herein to any specific commercial product, process, or service by trade name, trademark, manufacturer, or otherwise does not necessarily constitute or imply its endorsement, recommendation, or favoring by the United States Government or any agency thereof. The views and opinions of authors expressed herein do not necessarily state or reflect those of the United States Government or any agency thereof.**

## **DISCLAIMER**

**Portions of this document may be illegible in electronic image products. Images are produced from the best available original document.**

## SUMMARY

This literature review was prepared to support a study conducted by Pacific Northwest Laboratory (PNL, Project 16741) to assess the potential deposition and resuspension of radionuclides in the 291-Z ventilation exhaust building located in the 200 West Area of the U.S. Department of Energy's Hanford Project near Richland, Washington. The filtered ventilation air from three of the facilities at the Plutonium Finishing Plant (PFP) complex are combined together in the 291-Z building before discharge through a common stack.

Production in the PFP began in 1949. The purpose of the plant was to purify plutonium nitrate solution produced in the fuel separations facility and reduce the solution to plutonium metal. The other two facilities included in this review, which are part of the PFP complex, are the Plutonium Reclamation Facility (PRF) and the Waste Incinerator Building (WIB). The PRF was used to recover plutonium from wastes. The WIB was used to remove plutonium from contaminated solid wastes and reduce the volume of those wastes. The processes used in these facilities determine the composition of the aerosols released to the exhaust ventilation system. A timeline in Section 3.0 shows the operation of the facilities, changes made to the operations, and changes in the exhaust ventilation system. The timeline also includes a brief description of accidents or unusual events that may have released particulate material to the exhaust ventilation system. The main points found during this literature search are as follows:

- One of the weakest points in available data is the particle characterization.
- While deposition can be well characterized for modeling purposes, adhesion can be quantified only well enough to allow estimates of the relative importance of the different types of adhesive forces.
- Adhesion of the particles is strongly affected by the relative humidity of the airflow and the wall temperature, which control the near-wall humidity.
- Several of the aerosol samples taken in 1971 contained relatively small amounts of plutonium apparently bound to inert particulate.

- Estimates of deposition velocity show that for particles of 1- $\mu\text{m}$  AED and smaller, deposition is most affected by vapor motion toward the walls (if condensation is occurring), by temperature gradients (for walls cooler than the gas), and by diffusion.

## CONTENTS

1.0	INTRODUCTION . . . . .	1.1
2.0	POST HEPA VENTILATION DESCRIPTION . . . . .	2.1
2.1	PLUTONIUM FINISHING PLANT (234-5Z) . . . . .	2.1
2.2	PLUTONIUM RECLAMATION FACILITY (236-Z) . . . . .	2.3
2.3	WASTE INCINERATOR BUILDING (232-Z) . . . . .	2.6
2.4	FANHOUSE AND STACK (291-Z) . . . . .	2.6
2.5	SURFACE COATINGS AND VOLUMETRIC FLOW RATE . . . . .	2.7
3.0	PLUTONIUM FINISHING PLANT HISTORY . . . . .	3.1
3.1	PURPOSE AND USE OF FACILITIES . . . . .	3.1
3.1.1	Plutonium Finishing Plant . . . . .	3.2
3.1.2	Plutonium Reclamation Facility . . . . .	3.3
3.1.3	Waste Incinerator Building . . . . .	3.3
3.2	TIMELINE . . . . .	3.5
3.3	PREVIOUS MEASUREMENTS/CHARACTERIZATION OF PARTICLES . . . . .	3.7
4.0	DEPOSITION AND ADHESION . . . . .	4.1
4.1	ADHESIVE FORCES ON PARTICLES . . . . .	4.2
4.1.1	Total Adhesive Force . . . . .	4.2
4.1.2	Types of Adhesive Force - Dry Environment . . . . .	4.2
4.1.3	Types of Adhesive Force - Wet Environment . . . . .	4.4
4.1.4	Adhesive Forces - Miscellaneous Considerations . . . . .	4.6
4.1.5	Surface Roughness . . . . .	4.7
4.2	PARTICLE DEPOSITION IN DUCTS . . . . .	4.7
4.2.1	Deposition in Linear Flow . . . . .	4.9
4.2.2	Deposition in Bends . . . . .	4.10
4.2.3	Deposition With Temperature or Vapor Gradients . . . . .	4.11
4.3	PARTICLE REBOUND . . . . .	4.12
4.4	PARTICLE DETACHMENT . . . . .	4.13
4.5	DEPOSITION AND ADHESION IN THE Z-PLANT DUCTS . . . . .	4.16
4.5.1	Sizes of Z-Plant Aerosols . . . . .	4.16
4.5.2	Adhesion Mechanisms in Z-Plant Ducts . . . . .	4.18
4.5.3	Experiments Applicable to Z-Plant Resuspension . . . . .	4.18
5.0	CONCLUSIONS AND RECOMMENDATIONS . . . . .	5.1
6.0	REFERENCES . . . . .	6.1

FIGURES

2.1	Cutaway View of 234-5Z and 291-Z Building Ventilation Exhaust System . . . . .	2.2
2.2	Top and Side Views of 234-5Z Stack Manifold . . . . .	2.4
2.3	View of 291-Z Central Plenum, Fans, Ducts, and Stack . . . . .	2.5
3.1	Plutonium Reclamation Process Diagram . . . . .	3.4
3.2	Results of Hold-up Measurements . . . . .	3.9

## 1.0 INTRODUCTION

This literature review was prepared to support a study conducted by Pacific Northwest Laboratory (PNL, Project 16741) to assess the potential deposition and resuspension of radionuclides in the 291-Z ventilation exhaust building located in the 200 West Area of the U.S. Department of Energy's Hanford Project near Richland, Washington. The filtered ventilation air from three of the facilities at the Plutonium Finishing Plant (PFP) complex are combined together in the 291-Z building before discharge through a common stack. These three facilities contributing filtered exhaust air to the discharge stream are 1) the PFP, also known as the Z-Plant or 234-5Z, 2) the Plutonium Reclamation Facility (PRF or 236-Z), and 3), the Waste Incinerator Building (WIB or 232-Z).

The 291-Z building houses the exhaust fans that pull air from the 291-Z central collection plenum and exhausts the air to the stack. Section 2.0 of this report is a description of the physical characteristics of the ventilation system from the High Efficiency Particulate Air (HEPA) filters to the exhaust stack.

A description of the processes performed in the facilities that are vented through 291-Z is given in Section 3.0. The description focuses on the chemical and physical forms of potential aerosols given off from the unit operations. A timeline of the operations and events that may have affected the deposition of material in the ventilation system is shown. Aerosol and radiation measurements taken in previous studies are also discussed.

Section 4.0 discusses the factors that influence particle deposition and adhesion. Mechanisms of attachment and resuspension are covered with specific attention to the PFP ducts. Conclusions and recommendations are given in Section 5.0.

## 2.0 POST HEPA VENTILATION DESCRIPTION

The 291-Z building houses the fans that exhaust air from the PFP, PRF, and WIB to a 200-ft stack. Figure 2.1 is a diagram of 291-Z showing the fans, inlet ducts, stack, and basic structure. These facilities are described in the following subsections. Some of the factors important in determining the amount and characteristics of deposited/resuspendable material in the ventilation system are surface coatings, materials of construction, insulation or exposure to temperature fluctuations, obstructions to flow, bends, dead air spaces, changes in duct sizes, and other areas of flow variation. These factors are identified and discussed for each area. Other factors such as the chemical and physical properties of potentially deposited aerosol also influence deposition and resuspension. These are more process related and are discussed in Section 3.

### 2.1 PLUTONIUM FINISHING PLANT (234-5Z)

The PFP was built to convert plutonium nitrate to plutonium metal. The plant is divided into zones, with Zones 3 and 4 being the areas controlled for the processing of radioactive materials. The Zone 3 ventilation system exhausts air from processing areas, rooms, and hallways; the Zone 4 system exhausts glove boxes, process and laboratory vacuum systems, vaults, and hoods where highly radioactive material is stored and processed. These two zones are the most likely to contribute radioactive contamination to the ventilation system.

Zone 3 is shown in Figure 2.1 as E-3 depicted by a dotted line connecting filter rooms 311 through 316, and 318. The exhaust gases pass through automatic dampers as they exit the filter rooms, then travel through short lengths of metal duct into a stack manifold on the duct level (located between the first and second floors). Several 90-degree bends and changes in duct sizes are shown in Figure 2.1.

The exhaust from Zone 4, designated E-4 in Figure 2.1, passes through rooms 309 and 310. (Room 309 is the main filter room and 310 is an alternate). As the exhaust exits the Zone 4 filter rooms, it travels through automatic dampers, through short duct lengths, and down into the east side of the stack

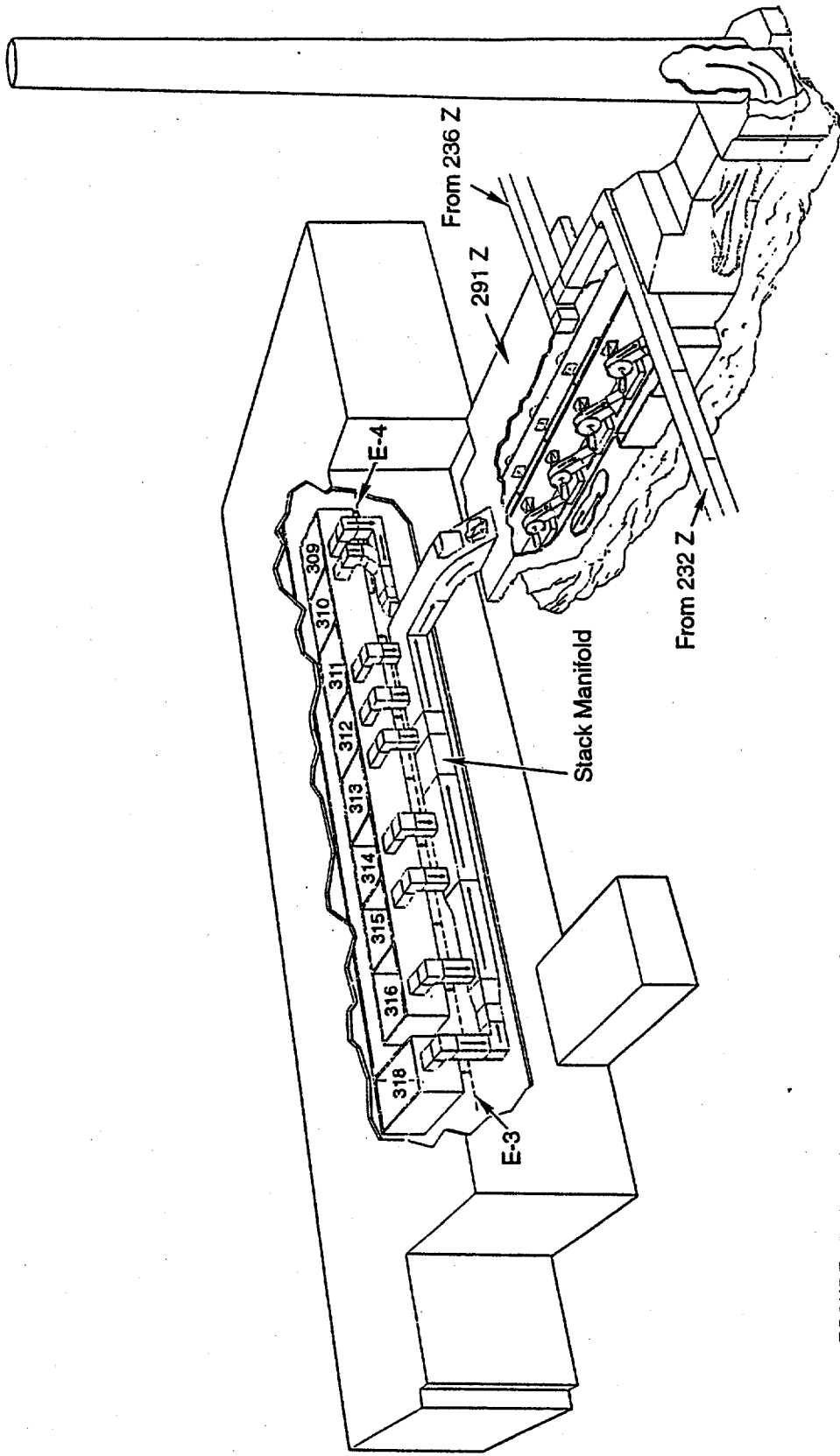


**FIGURE 2.1.** Cutaway View of 234-5Z and 291-Z Building Ventilation Exhaust System

manifold. Besides the 90-degree bends shown in Figure 2.1, the Zone 4 system also contains a flow straightener in its portion of the stack manifold.

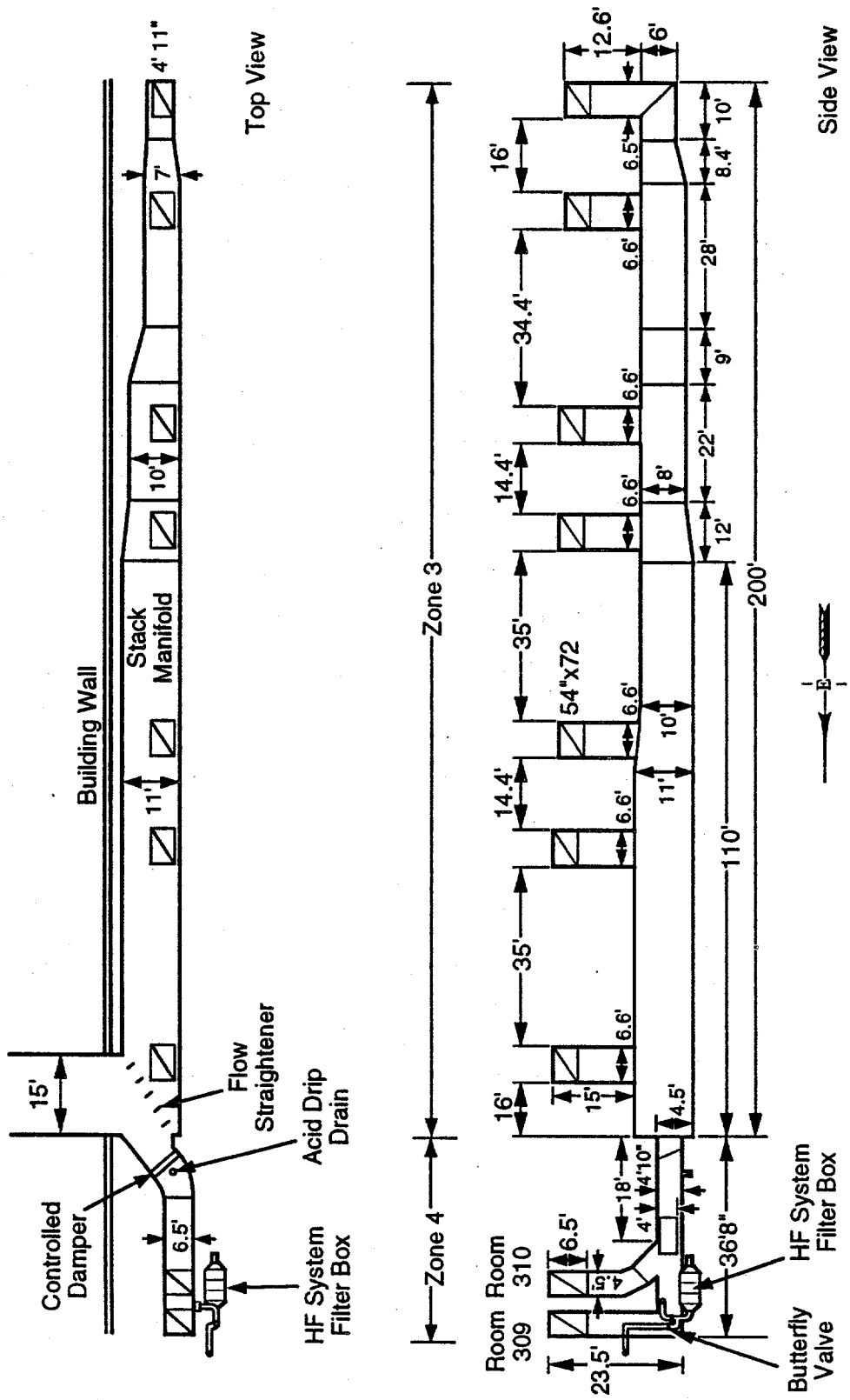
Top and side views of the stack manifold are shown in Figure 2.2. An acid-drip drain is identified downstream of the exhaust from 309 and 310 in Zone 4. The different duct sizes of the manifold in Zone 3 and a flow straightener where the stack manifold makes a 90-degree bend to exit the PFP are also depicted.

Hydrofluoric acid (HF) is used in an intermediate step in the conversion of plutonium nitrate to plutonium metal. Because HF is highly corrosive, a potassium hydroxide scrubber system was developed in the PFP to process off-gases. Scrubbed exhaust from the HF system was filtered by acid-resistant filters before discharging to the filter box and joining the Zone 4 exhaust shown in Figure 2.2.

Two butterfly valves allow HF system exhaust to either be routed to room 308, which is the outer room surrounding much of the ductwork on the second floor, or directly to the stack manifold. The exhaust routed to room 308 would then pass through the 309 or 310 filter rooms. The butterfly valves are normally positioned so that the exhaust from the filter box flows directly into the Zone 4 end of the stack manifold between rooms 309 and 310.

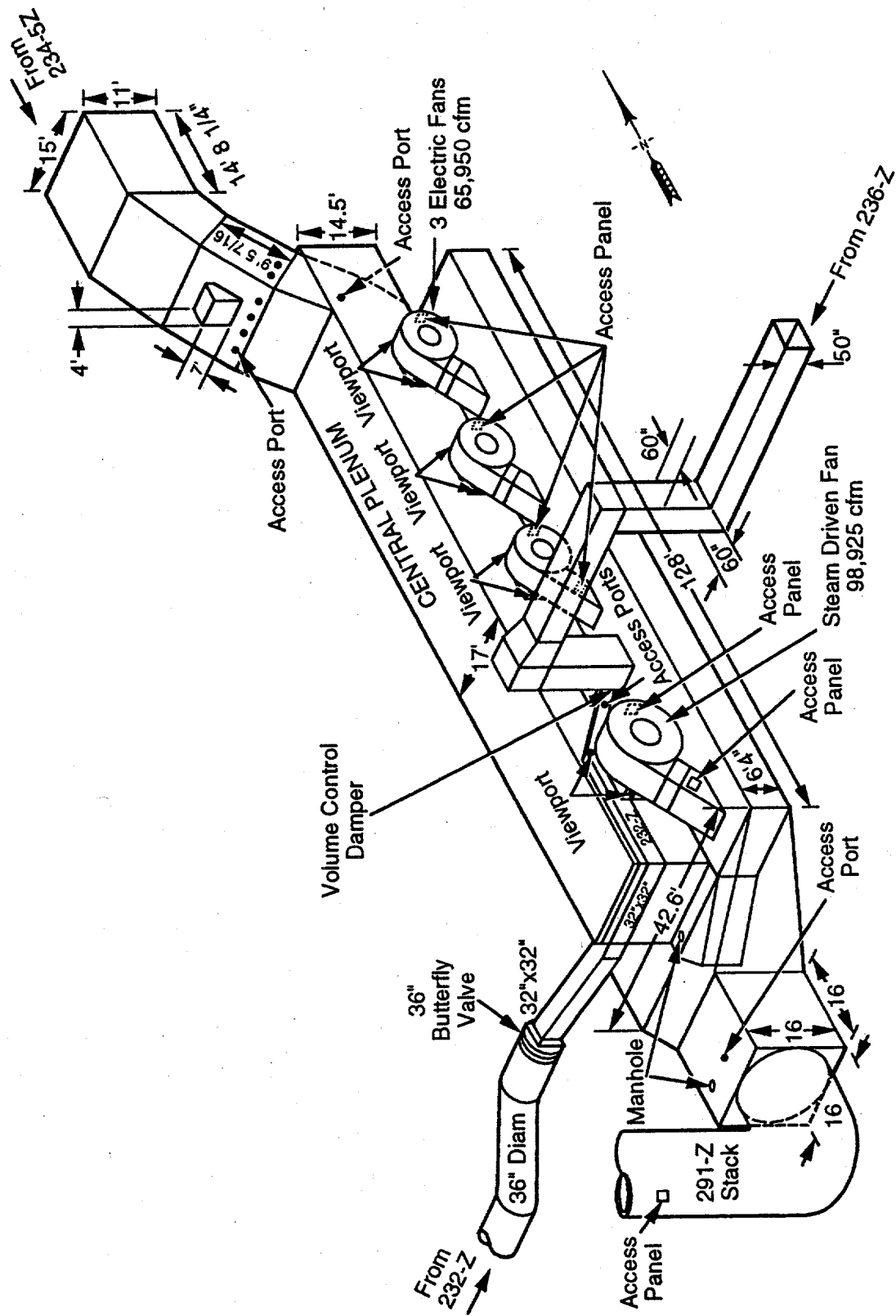
## 2.2 PLUTONIUM RECLAMATION FACILITY (236-Z)

The PRF was used to recover plutonium from wastes. Process exhausts from this facility were routed through a filter room and through a single duct to 291-Z. The duct runs underground until reaching the east side of 291-Z as shown in Figure 2.3. From there it runs over the roof of 291-Z to an access panel. It then runs down through the access panel and enters the east side of the central plenum at a location that was originally designed as an entry area for a replacement fan. A louvered damper is located as indicated on the diagram.



S9301061.2

FIGURE 2.2. Top and Side Views of 234-5Z Stack Manifold



2.5

FIGURE 2.3. View of 291-Z Central Plenum, Fans, Ducts, and Stack

S9301061.1

### 2.3 WASTE INCINERATOR BUILDING (232-Z)

The WIB (232-Z) was used to remove plutonium from and reduce the volume of contaminated solid wastes. The ventilation system downstream of the 232-Z final HEPA filters is composed of two cylindrical (2-ft-diameter) transiteducts that run below floor level to a single (3-ft-diameter) underground transite duct north of the incinerator building. A butterfly valve is located at the west wall of 291-Z where the transition occurs from a cylindrical duct to a 32-in. x 32-in. square metal duct.

As shown in Figure 2.3, the square duct runs alongside the top of the south side of the 291-Z central plenum, makes a 90-degree bend, and then descends to join with the portion of the 236-Z duct entering the central plenum. The 232-Z duct has recently been blanked off with a barrier inserted at the juncture of the 232-Z/236-Z ducts.

The duct from 232-Z has a number of 90-degree bends: where the two transite lines empty into one, where the square duct turns on the corner of the 291-Z building, and where the line enters the 291-Z main duct. A flow straightener is located where the duct corners in the 291-Z building.

### 2.4 FANHOUSE AND STACK (291-Z)

As described in earlier sections, ducts from the PFP, PRF, and 232-Z all enter into 291-Z. Figure 2.3 shows the different entry points. Exhaust from the three facilities enters a large (15-ft x 20-ft) central concrete plenum. Several stainless steel squirrel-cage fans located on both sides of this central plenum (see Figure 2.3) draw air from the central plenum and move the air into two lower plenums on each side of the central plenum below the fans. The two flows join together downstream of the fans into a V shape and then flow into the 291-Z stack.

Most of the 291-Z building is below grade (see Figure 2.1). The temperature inside the fanhouse does not fluctuate as much as the outside air throughout the year because heat is generated by the fans, and the building is insulated by its below-grade location.

The stack is a concrete structure 200 ft high with an inside diameter of approximately 16 ft. An access door is located near the base of the stack and

a sampling system with constant air monitors (CAMs) that alarm at preset levels and record samplers for data collection is located at the 50-ft level. Filters from the CAMs and record samplers are changed weekly; both instruments measure airborne particles.

## 2.5 SURFACE COATINGS AND VOLUMETRIC FLOW RATE

Information on surface coatings of the ducts is scant and is found primarily in design drawings. In the PFP the interior of the Zone 3 ducting was designed to be coated with one coat of asphaltum (Hanford Drawing H-2-16019). The Zone 4 stack manifold design specifications (Hanford Drawing H-2-16026) stated "interior surfaces to be sand blasted, welds smoothed and primed with Amercoat #44; after primer is dry apply three coats of #44 Amercoat<sup>(a)</sup> body and three coats of #44 Amercoat Sealer." After the HF release occurred in 1986 (see timeline in Subsection 3.2), the HEPA filters in the HF line were replaced, and paint in the Zone 4 stack manifold was seen to be degraded.

The duct connecting the PFP and 291-Z buildings was to have interior surfaces sandblasted and welds smoothed and painted with #44 Amercoat primer (Hanford Drawing H-2-16017).

The concrete underground duct from the PRF to 291-Z was specified to be painted with two coats of Amercoat 86 Prime and finished with two coats of Amercoat 33 HV.

Coatings on the 232-Z line and on the concrete plenums inside the 291-Z building are unknown. The stack was designed to have the entire interior surface receive two coats of paint.

A 1982 report estimated that flow through the 291-Z stack was 270,000 cfm, of which 68% came from the PFP Zone 3 exhaust, 13% from the PFP Zone 4 exhaust, 17% from PRF, 2% from 232-Z, and less than 1% from the PFP process vacuum and air sampling systems (Vogt 1982). The total flow and relative contributions from each of the facilities has changed throughout the life of the plant, and these estimates are more representative of the current flow rates.

---

(a) Ameron Protective Coatings, Brea, California.

### 3.0 PLUTONIUM FINISHING PLANT HISTORY

Examining the types of processes used and changes in operating conditions in the PFP, PRF, and WIB over the history of the plant may aid in determining the content of potential deposits on the system surfaces. This section begins with a general description of the processes that contributed aerosols to the exhaust gases while the plant was operational. A discussion of the off-gas handling systems and potential chemical species from each process are included. A timeline showing operation of the facilities, changes made to the operations, and changes in the exhaust ventilation system is provided in Subsection 3.2. The timeline also includes a brief description of accidents or unusual events that may have released particulate material to the exhaust ventilation system. Finally, data from past investigative studies or monitoring records can provide clues to the present state and quantity of material deposited in suspected areas of duct. Pertinent information from these past studies or records are identified.

#### 3.1 PURPOSE AND USE OF FACILITIES

The processes conducted in the three facilities (PFP, PRF, and WIB) that vent to the 291-Z building are briefly described here.

##### 3.1.1 Plutonium Finishing Plant

The PFP, also known as the Z-Plant or 234-5Z, started operation in 1949. The purpose of the plant was to purify plutonium nitrate solution produced in the fuel separations facilities and reduce the solution to plutonium metal. Prior to 1949, these solutions were shipped offsite for further processing. The PFP gave Hanford the ability to fabricate plutonium metal pieces onsite.

The main process steps for converting plutonium nitrate were as follows:

- Oxalic acid was added to the nitrate solution to precipitate plutonium oxalate.
- The slurry was filtered to remove soluble impurities, and the oxalate was calcined to form plutonium dioxide powder.
- Plutonium dioxide was converted to  $\text{PuF}_4$  by continuous contact with HF gas in the fluorinator.
- $\text{PuF}_4$  was mixed with calcium metal and iodine crystals, and heated in a reducing atmosphere to plutonium metal.
- The Pu buttons were pickled in nitric acid.

The PFP also housed support processes such as scrap recovery, sampling and analysis, and a development laboratory.

The characteristics of process-generated aerosols would depend on the unit operation and the handling of the off-gas. Plutonium was present in various forms in the process: nitrate solution, oxalate slurry, filter cake, oxide and fluoride powders, and metal. Of these, the fine powders would be most vulnerable to transport by air. Deposited particles may also have reacted with the deposition surfaces, chemical vapors, and deposited liquid aerosols. These reactions may have produced hard-to-disturb crusts or easy-to-disturb flakes. Vapors from chemicals used in significant quantity in the processes were probably available for reaction with process aerosols. These chemicals would have included hydrofluoric acid (HF), carbon tetrachloride ( $\text{CCl}_4$ ), tri-butyl phosphate (TBP), and water.

### 3.1.2 Plutonium Reclamation Facility

The PRF (236-Z) was built to reduce the amount of plutonium disposed of as waste. Waste was brought in from the PFP, WIB, or americium recovery (242-Z). Processing in the facility included dissolution of Pu, extraction, and stripping. Figure 3.1 is a flow diagram showing the basic components of the process.

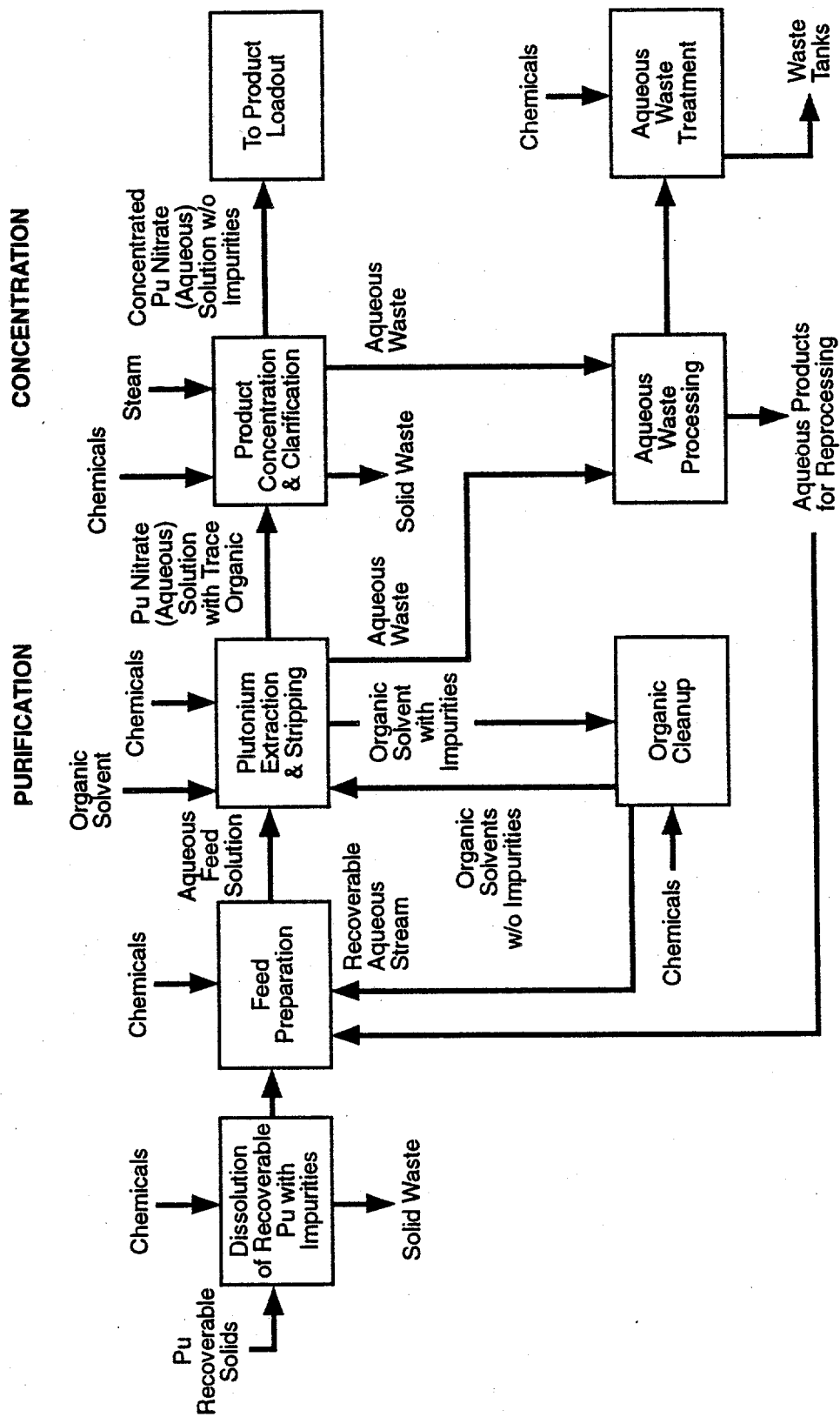
The process purified Pu from PFP process scrap and waste. The Pu in the scrap was converted to Pu(IV) nitrate by dissolution. Plutonium was then extracted into the organic phase and stripped back into acid solution via solvent extraction columns. The solution was then concentrated so that it could be sent to metal conversion in the PFP.

The PRF used a number of different chemicals, including  $\text{CCl}_4$  and TBP. Plutonium was present in a variety of liquid solutions. A high-humidity exhaust airflow was indicated based on the type of processes taking place in the facility. The dampness of the samples collected in 1971 (see Section 4) corroborated this supposition. The apparent salt content and oxidation of the sampling surfaces suggest that the acids and salts used in the PRF processes were present in the exhaust gases.

### 3.1.3 Waste Incinerator Building

The purpose of the WIB was to remove plutonium from contaminated solid waste. Glove boxes were used for sorting wastes, leaching plutonium from noncombustibles, and chopping and burning the combustibles. Off-gas was processed through a scrubber and filter system. Leaching and incineration were discontinued in 1973, but the sorting hood remained in use. Room air was exhausted through HEPA filters in the floor and the sorting hood was exhausted through one non-testable and one testable HEPA filter (Vogt 1982).

The scrubbing and leaching processes could have been a source of water vapor in the exhaust streams, which might have contributed to scale deposits or rust in the downstream ducts. Plutonium would have been present in the facility in the form of contamination on incoming waste, as a solution in the leaching process, and in ash after scrap incineration. The scrubber and filter system would have mitigated the release of plutonium-bearing ash particles into the exhaust ducts.



S9301061.5

FIGURE 3.1. Plutonium Reclamation Process Diagram

### 3.2 TIMELINE

Production in the PFP started in 1949 with the operation of the Rubber Glove Line, which continued operation until the Remote Mechanical Line was started up in 1953. Many projects for upgrading the facility, with regard to safety, enhanced capacity, and additional capabilities have been completed.

Startup and shutdown of operations, accidents, and other significant events are identified in the following timeline. Much of the information for the timeline was extracted from Schilling (1990) and Vogt et al. (1983). The timeline may not be complete because some information was unavailable due to the classification of operating documents.

- 1949 Startup of plutonium finishing in 234-5Z.
- 1953 Original process automated to reduce worker radiation exposure (Remote Mechanical A, RMA, line started up).
- 1955 Startup of Recuplex (236-Z), solvent extraction recovery of plutonium from finishing plant liquid waste.  
  
Modifications were completed to the fluorination and metal reduction steps of the RMA line for increased capacity.  
  
Additional process air-drying facilities were completed.
- 1958 New process equipment for PFP installed. Combustible exhaust filters replaced with noncombustible ones.
- 1959 Recuplex converted from semi-works to manufacturing facility.
- 1960 Second Remote Mechanical Line (RMC) started up.  
  
PFP vacuum system replaced.
- 1961 Startup of incinerator and leach facilities (232-Z) to recover plutonium from solid waste.
- 1962 Criticality accident in Recuplex; facility shutdown.
- 1963 Glove box ion-exchange process was set up to reprocess PFP liquid waste in the interim between Recuplex shutdown and PRF startup.
- 1964 Startup of PRF to replace Recuplex. Glove box pressurization caused by nitric acid reacting with Pu metal fines; off-gas system overwhelmed, resulting in a release through a roof vent.

- 1965 Americium recovery starts in 242-Z.  
Parts fabrication ceases at PFP.
- 1970 Continuous americium recovery system installed in 242-Z.
- 1971 Startup of plutonium oxide blending and production in PFP.
- 1972 Capability to separate Pu from U in mixed scrap started up in PRF.
- 1973 New recirculating off-gas scrubber installed for RMC fluorinator.  
Incinerator and leach facilities shutdown.  
RMC line placed on standby.
- 1976 Americium ion-exchange explosion; 242-Z americium recovery shutdown.  
234-5Z shutdown.
- 1978 Restart of 234-5Z operations.
- 1979 High stack release during a HEPA filter replacement in 232-Z, which dislodged filter or other surface contaminants.  
PRF placed on standby.  
RMA line and plutonium oxide production ends.
- 1980 Plutonium scrap can fire in PFP contaminates most of Zone 3 operating area.  
Americium recovery in 242-Z restarted.
- 1981 17-in. Hg vacuum line installed.
- 1982 Room 308 contaminated during filter change.
- 1984 PRF restarted. Campaigns in January 1984, July 1987.
- 1985 RMC line restarted in PFP. Six campaigns conducted from 1985 - 1989.
- 1986 Jan. 28 HF release caused destruction of HF system filters (PFP SAR Draft). PFP operations halted for nine-month period due to criticality-prevention specification violation.
- 1987 New 9AB filter box installed (HF system).
- 1989 April 5 HF release measured at 10 ppm HF at filterbox 9B

### 3.3 PREVIOUS MEASUREMENTS/CHARACTERIZATION OF PARTICLES

Samples have been taken of particulate material in the exhaust ventilation system for the PFP. In a study conducted by Mishima and Schwendiman in 1970 and 1971, samples were collected from the Zone 4 PFP exhaust, HF system, vacuum line, PRF, 232-Z, and 291-Z stack. Observations were as follows:

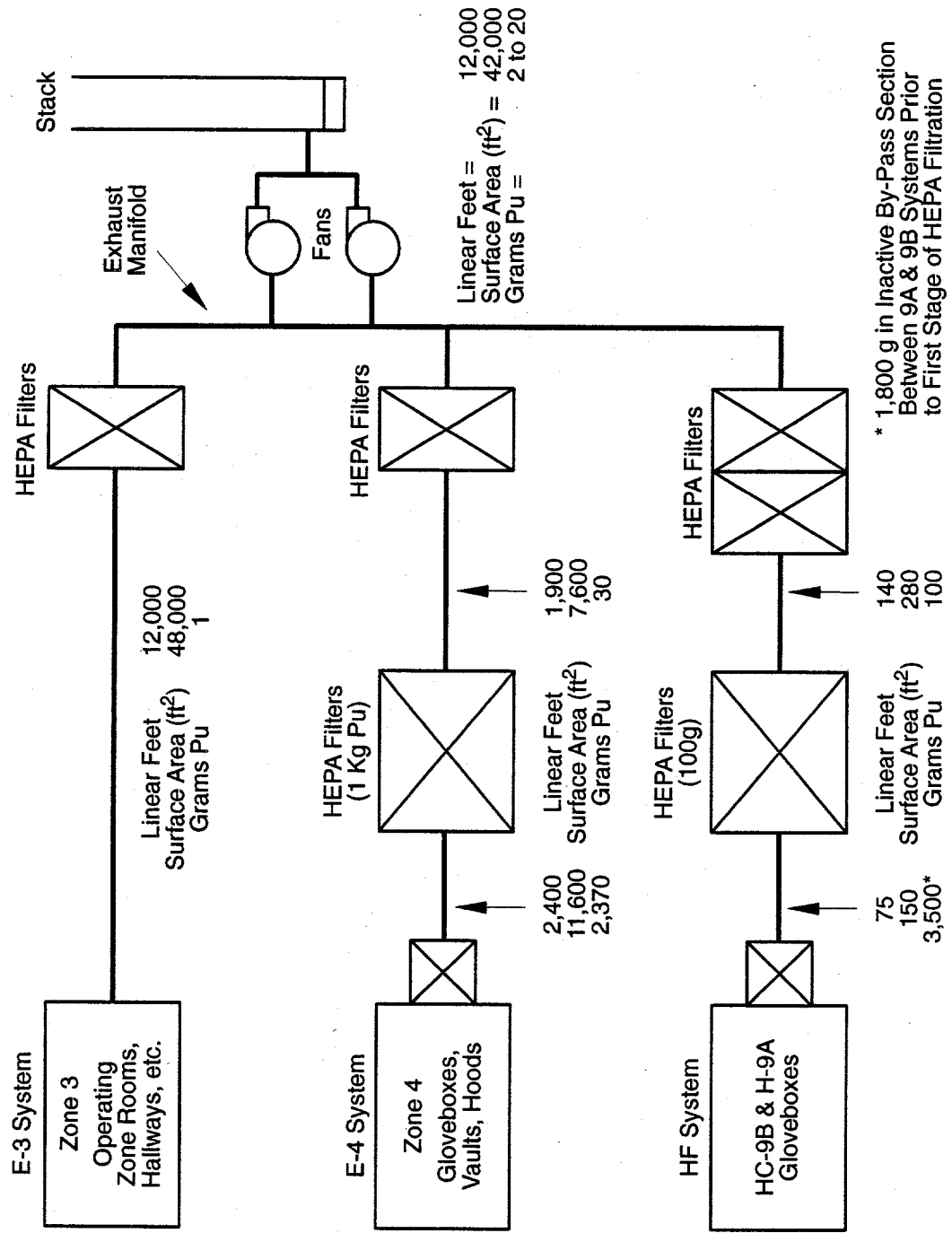
- In the plenum downstream of the 309 filter room, the calculated activity concentrations varied between  $4.5\text{E-}06$  and  $1.0\text{E-}03$  dpm/ft<sup>3</sup> (disintegrations per minute). The filtered material was "black with shiny patches," with measured aerodynamic median activity diameters (AMAD) of 9.5 and 20  $\mu\text{m}$ .
- The HF system exhaust was sampled in the winter (70-71). Samples were taken downstream of the final filter bank enclosure. An activity concentration of 0.06 dpm/ft<sup>3</sup> was measured. The AMAD of the particles was 7.4  $\mu\text{m}$ , but the activity distribution of the material was bi-modal, indicating more than one mechanism of particle formation.
- The vacuum system maintained at 26 in. Hg was sampled between October and December of 1970. Samples were taken from the line between the vacuum pump and the main exhaust plenum. All the interior surfaces and plates from the samples were loaded with a glassy, hard material resembling hard water deposits. An activity concentration of as high as 2.8 dpm/ft<sup>3</sup> was measured. The AMAD was estimated to be less than 1.6  $\mu\text{m}$  with a log-normal size distribution, indicating one mechanism of particle formation.
- The PRF building exhaust was sampled from a duct just upstream of the entry into the 291-Z exhaust plenum. "A large quantity of moist, reddish-brown, granular material was found on the filter sample ... and the rubber cement surface on impactor plates and impactor walls appeared oxidized." (Mishima and Schwendiman 1971, p. 18). The AMAD was 3  $\mu\text{m}$ . The coarseness of the material pointed to generation of the particles downstream of the filters. The material could have been rust from the existing duct, which was metal and aboveground. The sample was described as having a "high salt content" (Mishima and Schwendiman 1971, p. 18). The activity concentration was low ( $1\text{E-}4$  dpm/ft<sup>3</sup>). Since the sampling described here, much of this duct has been replaced with a concrete below-ground duct.
- The 232-Z duct was sampled during incinerator operations. The sample showed "highly active, coarse, red and gray particles" (Mishima and Schwendiman 1971, p. 11). The outlet for the sample was on a vertical wall of a sloped duct. The red coloring may suggest rust; gray may indicate ash. The AMAD was 8  $\mu\text{m}$ , with a log-normal distribution.

- The 291-Z stack was sampled at the base of the stack in the last quarter of 1970. Considerable condensation was noted and the sampled material was dark gray. The activity concentration was low,  $6.4E-03$  dpm/ft<sup>3</sup>. The plutonium was believed to be attached to inert particles.

A separate measurement program conducted from October 1972 to May 1973 sampled particles at the base of the stack (Mishima and Schwendiman 1973a). Seven sets of samples were taken. The AMAD from the samples ranged from 3.3 to 9.0  $\mu\text{m}$  with 60 to 80 percent of the activity associated with particles less than 10  $\mu\text{m}$ . The average activity was 0.034 dpm/ft<sup>3</sup>. No apparent correlation was seen between building operations and measured activity.

A study was performed in 1976-77 on the 291-Z stack to determine the adequacy of the in-place sampling system (Glissmeyer 1992). Samples were taken at the 50-ft level of the stack. All of the samples contained particles with the appearance of rust. The AMADs of plutonium-containing particles were between 3.5 and 8.6  $\mu\text{m}$ .  $\text{TiO}_2$  and ZnS tracers with aerodynamic mass mean diameters (AMMDs) of 1.3 and 8 to 9.5  $\mu\text{m}$  were released into the stack to test the air sampling systems.

An estimation of holdup in the PFP was reported in Schilling (1989). Nondestructive assay (NDA) data were collected from December 1986 through 1988 on ventilation ducting and process vacuum piping. In addition, physical samples were taken from the exhaust stack manifold in February 1988 while replacing the HF system filter box. Figure 3.2 shows the results of the data analysis. A later measurement of the exhaust manifold revised the surface area to 55,500ft<sup>2</sup> and the grams Pu to 2-20 (PFP Engineering Laboratory 1989).



S9301061.3

FIGURE 3.2. Results of Hold-up Measurements

#### 4.0 DEPOSITION AND ADHESION

In order for airborne material to become part of the "holdup" attached to the duct, it must first be moved to the duct walls (sides, top, or bottom) and then adhere to them. The two somewhat overlapping processes of deposition and adhesion are therefore relevant to the potential buildup of radioactive material in the Z-Plant ducts and stack. In deposition, airborne particles or droplets are brought to the duct wall. On contact with the wall, the particles either rebound or adhere. Even if the particle does adhere to the wall, it can subsequently be detached if the adhesion forces are not strong enough to hold it. If the particle is completely detached and returns to the bulk airflow, it is said to be resuspended; the greater the adhesion force is on a particle, the greater is the force required to resuspend it. It is also possible for a particle, on becoming detached, to remain in the flow boundary layer, be carried along the surface of the wall, and become reattached shortly thereafter; this is known as saltation.

The difference between rebound and detachment, and between resuspension and saltation, is to some extent a matter of the timing of particle detachment and reattachment. Thus the different processes may not be very well distinguished from each other either in theory or in experiment. Another ambiguity in literature data arises from the definition of deposition: deposition velocity may or may not be defined so as to include the effects of rebound and detachment. In general, experimental work is likely to measure a "deposition velocity" that does include the decrease in deposition that is associated with rebound and detachment. Theoretical work usually assumes "100% sticking" or zero rebound and detachment.

This section of the report will first discuss the forces that are available to hold particles to surfaces in the general case. Then the case of deposition and adhesion in a duct will be discussed, again without specific attention to the conditions in the Z-Plant post-HEPA exhaust ducts. Finally, the experimental data found in the literature that might be of use for the Z-Plant duct conditions will be given and conclusions will be derived from them.

## 4.1 ADHESIVE FORCES ON PARTICLES

### 4.1.1 Total Adhesive Force

The adhesive or autohesive force is the force required to detach a particle from a surface. By definition, particles that are in contact only with the surface, as in a monolayer, are undergoing adhesion, while particles in a layer that are only in contact with each other are undergoing autohesion. However, both adhesive and autohesive forces are controlled by similar physical mechanisms.

The adhesive force can be quantified in several different ways. The adhesion number is the fraction of particles detached at a given experimentally applied force (e.g., centrifugal, vibrational, or air drag). This is also referred to as "surface particle retention." The adhesive force for a given particle size range is often used to mean the force required for 50% detachment under the conditions of the experiment (Ranade 1987). A quantity that is loosely related to adhesive (or detachment) force is the resuspension fraction, the total fraction of attached material that is found to leave a macroscopic area over a given period of time as the result of applying some force (often not quantified). The literature also refers to "sticking coefficients", which are the fraction of particles (usually in an airflow) that become attached to a surface rather than rebounding from it.

In general, the total adhesion force, which is the sum of many different forces, increases approximately linearly as particle diameter increases while the particle weight force increases as the cube of diameter. In the particle size range from 10 to 1000  $\mu\text{m}$ , the weight and adhesive forces may be of the same order of magnitude, but for a 1- $\mu\text{m}$  particle the adhesive force can easily exceed the weight force by several orders of magnitude (Bowling 1985). The adhesive force can be made up of molecular, electrostatic, capillary, contact, and magnetic forces, depending on the properties of the materials and the medium.

### 4.1.2 Types of Adhesive Force - Dry Environment

Molecular (van der Waals) forces, electrostatic forces, and magnetic forces act before the particle has contacted the surface, both bringing the particle to the surface and establishing the contact area (often through

deformation of the surfaces). The molecular component of adhesion forces depends on the particle dimensions, contact area, and properties of the bodies. Of the forces that act at a distance, molecular forces predominate below 50- $\mu\text{m}$  particle size and electrostatic forces above; in the presence of surface asperities, electrostatic forces can also predominate for smaller particles. The distances over which these forces act are probably of the order of 0.01  $\mu\text{m}$  or less.

Molecular forces are always present and result from interactions between the induced and natural instantaneous dipoles in neighboring atoms. Although the theory of these interactions is highly developed, it does not lend itself to application: for example, the effects of microroughness and deformation, as well as trace impurities, are not readily definable for a given application but drastically affect the van der Waals force. For a 5- $\mu\text{m}$  sphere and a flat surface at a separation of 0.4 nm, the van der Waals force can range from less than 1 to more than 10,000 mdyn, depending on the medium, the molecular interaction properties of the materials, and the material hardness (Ranade 1987). The force is proportional to particle diameter, but a 2% deformation of the particle more than doubles the adhesive force (Bowling 1985).

Electrostatic or Coulombic forces arise from non-zero net charges on the particle and substrate. This is equivalent to an electrostatic interaction between the particle and its "image." Coulombic forces (or bulk excess charge image forces) require preliminary charging of the particle and typically decrease with time after contact owing to charge leakage, with more rapid leakage for higher electrical conductivity. Coulombic forces are proportional to the square of the particle diameter (Bowling 1985). They are eliminated by the presence of liquid.

In some cases, particles can acquire an electric charge through friction with the walls; this is known as triboelectricity. Minerals such as quartz, talc, starch, calcite, gypsum, hornblende, and sulfur (among others) display this property. The acquisition of net charge increases the adhesive force caused by Coulombic forces. The charge decreases with diameter and may increase or decrease with temperature, depending on the effect of the increased temperature on electrical conductivity of the particles and surface,

internal ionization, and moisture condensed on the particle. These properties are typically material-dependent (Zimon 1969).

After contact, several phenomena that determine contact area come into play. The pressure on the contact area induced by molecular forces can be from  $0.2\text{E}+09$  to  $3.0\text{E}+09$  dyn/cm<sup>2</sup>, and can produce increasing deformation and contact area with time. The greatest forces of adhesion therefore tend to occur for soft material bound to a metal, and hard oxide layers on metals reduce the force of adhesion. Simultaneous oxidation of a particle and a surface can cause the particle to become entrapped in the oxide (Bowling 1985). Sintering, diffusion, condensation, surface dissolution and alloying, capillary forces, and creation of solid bridges between particle and surface (as by melting) also affect the adhesive contact area. Capillary forces come about when a liquid meniscus is present between the particle and surface. Forces coming from "tackiness" of a surface film, such as a film of oil, typically depend on the rheological properties and thickness of the film.

#### 4.1.3 Types of Adhesive Force - Wet Environment

Capillary forces operate when particles are held by the surface tension and by the reduced pressure below the meniscus of the liquid that condenses in the gaps between particle and surface. The capillary force is negligible below about 65% relative humidity. Above 65% relative humidity, large increases in particle retention were found to occur in a 1-hour humidity exposure period, such that even particles in the 50- to 140- $\mu\text{m}$  (geometric) range were substantially retained. Total particle retention was above 80% after 100 h exposure at 84% relative humidity, and was 100% after 1 h exposure at 100% relative humidity. The non-capillary forces were estimated to contribute about 20% of the total particle retention (Whitfield 1979). Capillary forces are proportional to surface tension and so are lower for organic liquids than for water. For the same reason, capillary forces for water have the most effect on a hydrophilic surface and their least effect on a hydrophobic surface (Zimon 1969; Bowling 1985). Capillary forces are proportional to particle diameter. For a 1- $\mu\text{m}$  particle in water, the force is about 40 mdyn (Ranade 1987).

Another effect of the presence of water occurs when particles are brought to a surface in drops of water, or are trapped on a surface by drops of water. In these cases the adhesion number varies very little with particle and drop size for normally directed detaching forces. In this case the hydrophilicity of the surface is the main influence: removal from a hydrophilic surface is more difficult than removal from a hydrophobic surface. A tangentially directed force causes the drop to spread; hence particles of any given size are less easily detached as drop size increases. Smaller particles are less easily detached than larger ones, and the hydrophilicity of the surface is about as important as particle size (adhesive force increases as hydrophilicity increases).

After the water drop evaporates, the particles that were situated in it will require larger detaching forces than if they had settled freely onto the dry surface. This apparently results from a crust of non-volatile contaminants in the liquid that remains after the liquid has evaporated. The strength of adhesion after evaporation of salt solution droplets was higher for higher original (pre-evaporation) salt concentrations. Particles that had adhered where a drop had evaporated were almost not removable in an airflow of velocity less than 11 m/s. Even salt concentrations as low as 0.01% could produce 90% particle retention, compared to 60% retention for pure water (Zimon 1969). The adhesion of about 1% of the dust that was in a water drop, after the drop evaporates, becomes very strong; this results from the soluble, and so crust-forming, material. The adhesive force for the strongly bound particles can be on the order of 100,000 times the adhesive force for the other 99% of the particles (Williams and Nosker 1985). Deliquescent salts can also exhibit this behavior. Several common salts (carbonates, sulfates, and chlorides) have critical relative humidity levels ranging from 15 to 97%. The critical values are those at which a deliquescent salt takes up moisture to form a solution with uptake continuing until the vapor pressure of the solution is equal to that of the water vapor in the atmosphere above the solution.

A film of oil or other "tacky" substance can also effectively increase the contact area between the particle and surface. For a range of oil-film thicknesses, the adhesive force is maximum and does not vary with oil-film thickness; for thicknesses greater or less than that, adhesive force

decreases. Particle adherence to tacky films is not well quantified, although it is believed to depend on the viscosity of the film and the depth to which it is penetrated by the particle. In one case, the maximum adherence to an oil film occurred between 0.25 and 2 mg/cm<sup>2</sup> oil. For an oil film of density 0.5 mg/cm<sup>2</sup>, there was 80 to 100% retention of glass particles of diameter 5 μm or greater on an oily surface that was parallel to an airflow of 25 m/s (Zimon 1969).

#### 4.1.4 Adhesive Forces - Miscellaneous Considerations

Another area-affecting phenomenon present when particles in an airflow contact the sides of a conduit is associated with melting of the particles by friction heating. Some of the materials that are sensitive to the temperature increase caused by friction are those with low melting or softening points (e.g., waxes, fats, sulfur, and starch sugar) and dusts containing those materials. At low velocities these temperature-sensitive particles behave like the insensitive ones, first adhering and then rebounding as velocity increases. At higher velocities the melting or softening point is reached in the contact area, increasing adhesion and even welding particles to the surface. Finally, the velocity increases to the point that melting does not hold the particles and they begin to rebound again (Zimon 1969). Thus, particle retention that is affected by melting passes through two maxima.

Once contact is made and the particle area is established, short-range interactions such as chemical and hydrogen bonds can affect the adhesive force. Electrical double-layer forces (those arising from electrostatic contact potentials) are proportional to the area of contact and are greatly reduced by the presence of liquid in the gap. Adhesion of polymers has also been shown to be controlled by the acid or base nature of the surfaces; in addition, polar and metallic bonds can affect adhesion (Ranade 1987). All of these forces have different dependencies on particle size. The Coulombic pre-contact and capillary post-contact forces, when present, are often much greater than the molecular pre-contact or double-layer, post-contact forces.

Electrical double-layer (or contact potential) forces arise when particles contact a substrate and the charges on the particle surface induce an equal and opposite charge on the substrate surface. This type of

electrostatic interaction arises from the difference in the work functions of the materials, producing a contact potential. The double-layer adhesive force is greater for a grounded substrate than for a charged substrate. In addition, the electrical conductivity of the bodies that come into contact determines the adhesive force. Particles coming into contact with a semiconductor experience stronger adhesive forces than particles contacting a conductor (such as a metal). A layer of paint on metal is a semiconductor; both its conduction characteristics and its thickness can affect the double-layer adhesive force it exerts (Zimon 1969). At the maximum contact potential of 0.5 V and a separation distance of 0.4 nm, the electrostatic double layer force on a 1- $\mu\text{m}$  particle is about 1 mdyne (Ranade 1987). The double-layer force is proportional to particle diameter.

#### 4.1.5 Surface Roughness

Because all of the types of forces of adhesion depend on the area of contact between a particle and surface, or on the distance between the particle and the surface, surface roughness has an effect on adhesive force. A deformable material can provide more contact area (for a particle pressed onto it) and so increase adhesion. If the heights of the surface roughness are of similar or larger size than particle dimensions, contact area and adhesive force increase (compared to a perfectly flat surface). If the surface roughness is an order of magnitude smaller than particle dimensions, contact area and adhesive force decrease. This is illustrated by one case of particle detachment by an airflow: for particles of 20- $\mu\text{m}$  diameter, the detachment velocity was increased by increasing surface roughness, but the roughness had no effect on the detachment velocity for particles over 50  $\mu\text{m}$  in size. The surface roughness in these experiments was not stated (Zimon 1969).

## 4.2 PARTICLE DEPOSITION IN DUCTS

Deposition is the process controlling the transport of aerosols from the bulk airflow to the duct wall, where forces of adhesion can act on the aerosol. The several deposition mechanisms of interest are Brownian and turbulent diffusion, sedimentation (gravity deposition), inertial impaction, thermophoresis (present for a radial temperature gradient), and diffusiophoresis (which occurs during condensation of a vapor). Deposition can be described in

terms of a deposition efficiency or fraction of airborne material deposited in a length of duct. More commonly, the parameter "deposition velocity" is used; this velocity, when multiplied by the concentration of aerosol, gives the deposition rate per unit area or deposition flux. If the deposition velocity is constant in a given duct, then the deposition efficiency and deposition velocity are related as follows (Sehmel 1968):

$$\ln( C/C_0 ) = -4 \times ( K / V ) \times ( L / D )$$

Here C is the concentration a distance L downstream from where the original concentration  $C_0$  was measured, K is the deposition velocity, V the bulk flow velocity, and D the duct diameter. Deposition efficiencies depend on the length of duct and on the deposition velocity, which depends on the flow conditions and particle characteristics.

Both Brownian and turbulent diffusion affect particle deposition. In Brownian diffusion there is a net flux of particles toward surfaces because of concentration gradients produced by particle capture at the surface. Both the particle diffusivity and the fluid flow pattern past the surface affect deposition by diffusion (Chan et al. 1989). For a 2- $\mu\text{m}$  aerodynamic equivalent diameter (AED) particle, the effect of Brownian diffusion is important only below 0.3 m/s flow velocity; for a 0.1- $\mu\text{m}$  particle, Brownian diffusion can be important at flow velocities as high as 10 m/s. The effect of Brownian diffusion in turbulent flow diminishes with increasing particle diameter raised to the 1.5 power (Beal 1970). Turbulent diffusion is produced by the eddies in turbulent flow, and in typical bulk turbulent flows it dominates over Brownian diffusion for particles of 5- $\mu\text{m}$  AED or greater. However, in deposition Brownian diffusion remains an important consideration because turbulence decreases in the laminar boundary layer near the surface and Brownian diffusion dominates (Ounis and Ahmadi 1990). Turbulent and Brownian diffusion can produce deposition on the top and walls of conduits as well as the bottom.

Sedimentation of particles of 70- $\mu\text{m}$  AED or less follows Stokes' Law, which describes viscous-controlled gravity settling. The particle deposition velocity is proportional to particle diameter squared (or to particle area),

particle density, and the inverse of the fluid viscosity. For particles above 70- $\mu\text{m}$  AED, a Reynolds-number (#Re) dependent coefficient is used to correct the Stokes' Law deposition velocity (Chan et al. 1989). The slope of the surface upon which particles settle is also significant. Only 50% of freely falling glass particles of diameter 90, 70, 40, and 15  $\mu\text{m}$  adhered to a perchlorvinyl enameled surface at slopes of 10, 22, 42, and 48 degrees from the horizontal, respectively. This information on limiting slope does not pertain to particles less than about 10- $\mu\text{m}$  AED, since these do not fall vertically so much as they are carried by inertial and diffusion mechanisms (Zimon 1969). Particles deposited by sedimentation are typically found within a small angle of the bottom of conduits.

#### 4.2.1 Deposition in Linear Flow

In linear turbulent flow at sufficiently high velocities, inertial deposition (or impaction) occurs when particles "coast" on momentum to reach surfaces. For a 2- $\mu\text{m}$  AED particle in a tube a few centimeters in diameter, this effect becomes important above 0.3 m/s flow velocity, at which point the deposition velocity is  $1\text{E-}6$  m/s. For a 0.1- $\mu\text{m}$  particle, a flow velocity above 10 m/s is needed (and the resulting deposition velocity is about 0.0002 m/s). The inertial deposition velocity increases with particle diameter, but at an ever decreasing rate until finally size has no more effect. For an airflow velocity of 10 m/s, this size cutoff occurs at about 1-2  $\mu\text{m}$  (and a deposition velocity of 0.08 m/s). This neglects the effect of sedimentation (Beal 1970; Liu and Ilori 1974). The deposition of 1- to 28- $\mu\text{m}$  particles on the walls of vertical tubes, in which sedimentation plays no part, has also been tested. At the laminar-turbulent flow regime boundary or a #Re of about 2000, the deposition velocity was low ( $1\text{E-}06$  m/s). The deposition velocity increased with turbulence, up to on the order of 0.1 m/s at a #Re of about 50,000. Under these turbulent conditions in smooth tubes, deposition was shown to be higher near the inlet, outlet, and tube joints (Sehmel 1968).

#### 4.2.2 Deposition in Bends

In flow in a bend, deposition is controlled by centripetal force as well as the forces affecting linear flow. Flow tends to skew toward the outside of the bend; that is, the peak axial velocity is found on the outer side of the centerline. Recirculation in a plane perpendicular to the flow direction also occurs; the center of the recirculation is between the top and the inner side of the tube. The centripetal acceleration caused by the curve, and the recirculation, both increase the deposition in a bend compared to a straight conduit.

In horizontal bends, inertial deposition is controlled by the ratio of the bend curvature radius to tube radius (curvature ratio), the Dean number ( $\#De$ ), and the Stokes number (which is proportional to the particle diameter squared, the particle density, and the inverse duct diameter). The Dean number is the Reynolds number -  $\#Re$  - divided by the square root of the curvature ratio. The  $\#De$  is a direct measure of skewing and recirculation, and higher skewing and recirculation are linked with higher deposition. Experiments and analysis showed that for a tight 90-degree bend at high  $\#De$ , the area where impaction was likeliest to occur was the outside of the turn; for a loose turn at high  $\#De$ , inertial deposition was much more generally distributed. In general, the tighter the turn and the higher the  $\#De$ , the earlier in the bend most deposition occurred in terms of the angle traversed (Tsai and Pui 1990).

In vertical tube bends, there was found to be a Stokes number (for a given particle size) at which there was a minimum deposition efficiency. This resulted from an increase of deposition in the bend at smaller Stokes numbers because of increased sedimentation effectiveness; i.e., the lower flow velocity allowed gravity more time to deposit aerosol in the bend. There was also an increase of deposition at larger Stokes numbers because of inertial impaction. For bends that started from the horizontal and turned downward, deposition was roughly uniform along the entire angle traversed by the bend (Balashazy et al. 1990).

When flow passes around an obstacle, deposition is maximum on the front and back of the (cylindrical) obstacle and virtually zero at the flow

tangents, with the maxima much greater for low (5 m/s) than for moderate (14 m/s) velocities. The front of the cylinder accumulates particles up to 20  $\mu\text{m}$  in diameter, while the maximum diameter of particle adhered to the back is less than 10  $\mu\text{m}$ ; this distinction between front and back decreases with increased velocity. The number of particles deposited on front and back are roughly equal. It is also the case for plates in an airflow that the larger particles are a greater proportion of the deposit for angles closer to perpendicular to flow (Zimon 1969).

#### 4.2.3 Deposition With Temperature or Vapor Gradients

In thermophoresis, particles experience a radiometric force when they are suspended in a gas in which there is a temperature gradient. The drift velocity is proportional to the gradient and toward the cool surface. The effect of walls that are cooler than the gas is to enhance deposition, while warmer walls decrease deposition. The effect increases as heat transfer to and through the wall increases (Postma 1961). It follows that thermophoretic deposition is heaviest where the wall is coolest. Thermophoresis is not dependent on particle size, but does depend on the thermal diffusivity of the particle material (Davies 1966).

Diffusiophoresis occurs when condensation of vapor onto surfaces causes particle drift by two mechanisms. First, a net flow of gas toward the cool surface, or Stephan flow, convects particles with it toward the surface. Second, the gradient in water vapor concentration causes a molecular weight gradient that impels particles in the direction of the gradient or away from the surface. Stephan flow typically predominates. The particles that are convected toward the surface are scrubbed by the condensing vapor (Chan et al. 1989). Because condensation occurs on the coolest parts of conduit walls, diffusiophoretic deposition is heaviest there; however, the condensation may very well carry the particles to the bottom of the conduit. Diffusiophoresis is not dependent on particle size or shape, so long as the particle diameter is well above the mean free path of the air molecules, which is about 0.1  $\mu\text{m}$  at standard conditions (Davies 1966).

### 4.3 PARTICLE REBOUND

Rebound occurs immediately upon contact between a particle and a surface; detachment occurs some time after the particle has become attached. Detachment can lead either to resuspension of the particle into the bulk flow or to saltation, in which the particle remains in the surface layer. In saltation of soils, deposited particles between 100 and 500  $\mu\text{m}$  in diameter are taken up by the airflow to heights not exceeding 1 cm. They travel several cm downwind and on impact induce movement by, and possibly resuspension of, other particles. Transport via saltation tends to be temporary and short-range, while resuspension allows relatively long-range transport.

Because particles can rebound from a surface after impact, not all particle-surface contact leads to adhesion. The fraction of particles that rebound from the wall acts as a kind of "anti-deposition" mechanism. This effect is often included in experimental deposition velocities because of the difficulty of separating the two mechanisms experimentally. For example, one test showed maximum apparent deposition velocities for particles of about 30- $\mu\text{m}$  diameter at #Re of 10,000 to 20,000, and decrease of deposition at higher Reynolds numbers (Forney and Spielman 1974). In another set of tests, deposition of particles of 1- to 28- $\mu\text{m}$  size declined after #Re = 50,000, apparently because of particle rebound or resuspension (Sehmel 1968). In both cases, a sticky coating increased the apparent deposition velocity at high #Re by about an order of magnitude. In general, particles that arrive with kinetic energy will bounce off if the kinetic energy exceeds the energy of adhesion plus the energy lost in elastic and/or plastic deformation of the particle and the surface.

It follows that for a given particle size, there is in theory a critical velocity above which the particle will rebound from the surface and adhesion is not possible. As one example, quartz particles 2  $\mu\text{m}$  in diameter bounced off a smooth quartz surface for particle (or surface) velocities greater than 0.1 to 0.15 m/s (Zimon 1969). For metal and glass particles dropped onto metal and glass surfaces, the maximum velocities at which adhesion could occur were found to be dependent on the elastic or plastic deformability of the materials. As long as one of the metals was copper (relatively low yield limit), the maximum velocity of adhesion was relatively high -- 1 to 2 m/s for

10- $\mu\text{m}$  particles and 0.1 m/s for 20- $\mu\text{m}$  particles in copper/glass tests, or 2 m/s for 18- $\mu\text{m}$  particles and 0.3 m/s for 32- $\mu\text{m}$  particles in copper/steel tests. For steel/glass tests, in which the yield limits of both materials were considerably higher, the maximum velocities of adhesion were much lower, 0.05 to 0.09 m/s for particles under 10  $\mu\text{m}$  in size (Rogers and Reed 1984). Once above the limiting velocity, rebound can be overcome only at velocities high enough to make the particles penetrate the surface. For hard substances such as metals and oxides, penetration does not occur below velocities of several hundred meters per second (Zimon 1969).

In a study that did not distinguish between rebound and resuspension, the "stickiness" of aerosols released from the stack of a boiling water reactor (BWR) nuclear power plant were studied. These aerosols were found to have an AMAD of about 10  $\mu\text{m}$  "with large variations." These aerosols, which contained a variety of fission and activation products, were collected both on "sticky" coated rods and on dry, clean, stainless-steel rods. The ratio of material collected on the two sets of rods was about 10 to 1. This led the authors to speculate that at least 90% of material deposited on the rods was resuspended in the absence of stickiness and in the 20-50% humidity range where capillary forces had little effect (Strom 1988). The airflow velocity for the particle collection was not stated.

#### 4.4 PARTICLE DETACHMENT

Detachment (and resuspension) of dust on a surface exposed to airflow is the remaining mechanism of importance. Surface dust is acted upon by the adhesive force, the particle weight, the frontal force exerted by the flow on the particle, and the lift force (usually the least significant). The particle becomes detached when the frontal force exceeds the frictional force that is produced by the net downward force on the particle. The frontal force depends on the thickness of the boundary layer, which is laminar for bulk turbulent flows of less than 100 m/s velocity. For a laminar boundary layer whose thickness exceeds the particle diameter and whose velocity profile is linear, Stokes' Law can be used to approximate the frontal force. The force is thus proportional to the velocity in the boundary layer, inversely

proportional to the layer thickness, and proportional to the square of the particle diameter. At velocities less than 25 m/s, particles smaller than 50- $\mu\text{m}$  diameter are within the laminar boundary layer and so subject to Stokes' Law frontal forces. As the flow becomes more turbulent and the boundary layer thinner, lower bulk flow velocities are needed to detach a given particle. A range of detachment velocities can be observed for particles of the same size apparently under the same conditions (Zimon 1969).

An airflow around a dusty obstacle detaches particles to an extent that depends on the angle between the flow and the surface, not just on the air velocity. Maximum detachment of particles occurs at points of maximum velocity, where the flow is parallel to the curved surface of the obstacle. Only a small number of particles are detached from the front surface against which the air blows (producing a stagnation point), and even fewer are detached from the back (Zimon 1969).

As the flow velocity increases, fewer large particles stick to a surface because the increase in rebound (kinetic energy) and detaching force exerted by the airflow more than make up for the increase in inertial impaction. The elastic rebound force and the airflow (frontal) detaching force both increase as the square of particle radius, while the adhesive force increases only as the particle radius. By the same token, the lower kinetic energy for fine particles makes a high adhesive force (to overcome elastic rebound) less important to particle capture. Because less adhesive force is needed for particles with lower kinetic energy, there was little difference at low velocities in the deposition coefficients of wet and dry surfaces: for 20- to 60- $\mu\text{m}$  particles, the difference first appeared at about 2.3 m/s. For the same reason, the difference between wet and dry surfaces was less for fine (20 - 30  $\mu\text{m}$ ) than for coarse (50 - 60  $\mu\text{m}$ ) particles (Zimon 1969).

When more than a monolayer of adherent dust is present, the manner of removal of particles depends on whether adhesive forces are greater than autohesive forces (in which case erosion occurs) or autohesive greater than adhesive (in which case denudation occurs). In erosion, the topmost particles are first to be removed by airflow and are not raised far above the surface; if the adhesive forces are strong enough, the monolayer that finally remains is not stripped away. (This last is the case for room dust, carbonates, and

some gypsums.) In denudation, detachment occurs at the leading edge of the boundary between the surface and the dust layer, and a dust cloud fills the entire flow area.

As a general rule, the detachment velocity required to remove autohered particles is always less than that for adhered particles. As an example of the order of magnitude of autohesion detachment velocities, sandy soil particles of all sizes remained adherent to a plane glass surface for airflows below 4 m/s. Above that, the adhesion of the large particles diminished, although particles less than 1  $\mu\text{m}$  in diameter adhered even at 15 m/s air velocity. A velocity of 4 m/s was observed to be sufficient to detach an autohered layer of magnetite dust less than 10- $\mu\text{m}$  diameter, and in other cases velocities of between 3 and 10 m/s sufficed to entirely remove autohered layers of mineral dusts with sizes in the 20- to 90- $\mu\text{m}$  range. These air velocities almost certainly would have been inadequate to remove the adhered monolayer, however. An adhered layer of glass particles under 100  $\mu\text{m}$  was less than 30% removed from a horizontal plane surface by an air velocity of 11 m/s; the same conditions removed less than 10% of an adhered layer of particles under 50  $\mu\text{m}$  (Zimon 1969). Although autohesion detachment velocities are lower than those for adhesion, the two types of detachment velocities are of the same order of magnitude.

Detachment always requires an airflow velocity that is higher than the velocity above which sedimentation is minimized. Thus there is a range of buffer velocities, meaning that particles of a given size deposited at a given airflow require large, not slight, increases in velocity to be removed. The detachment velocity (minimum velocity needed to detach an adhered particle) depends on the adhesive and weight forces to be overcome. For particles larger than about 100  $\mu\text{m}$ , the adhesive force is negligible compared to the weight. Because the frontal force increases as the square of particle diameter while the weight increases as the cube, the detachment velocity increases with particle diameter above 100  $\mu\text{m}$ . Below 70- $\mu\text{m}$  diameter, adhesion (or autohesion) is more significant. Smaller particle sizes, particularly under 50  $\mu\text{m}$ , are not easily removed by airflow because of their higher adhesive forces. As an example, for corundum on an iron surface in a 10-cm tube, the detachment velocity was 11.4 m/s for 70- $\mu\text{m}$  particles, 10.6 m/s for 100- $\mu\text{m}$

particles, rising to 16.3 m/s for 1000- $\mu\text{m}$  (1 mm) particles. As another example, airflows of 11 m/s or less removed 10% or less of glass particles less than 50- $\mu\text{m}$  diameter from a horizontal surface; on the other hand, removal was substantially complete for particles in the 100- to 150- $\mu\text{m}$  range (Zimon 1969).

#### 4.5 DEPOSITION AND ADHESION IN THE Z-PLANT DUCTS

Deposition and adhesion depend on the properties of the aerosol, the surface on which it collects, and the flow carrying it. The aerosol in the Z-Plant post-HEPA ducts probably consists of plutonium oxides, fluorides, oxalates, and possibly nitrates. Any and all of this material may be associated with high relative humidity, soluble salts, acids, or (in the case of the 236-Z exhaust) organic solvents such as TBP and carbon tetrachloride. The surfaces in the ducts are mostly coated metal or concrete, although a considerable length of the 232-Z duct is Transite. Flow conditions are uniformly turbulent because of the large duct diameters and 4- to 7-m/s air velocities. The airflow passes through bends, dampers, butterfly valves, flow straighteners, and the blades of the exhaust fans.

##### 4.5.1 Sizes of Z-Plant Aerosols

Existing documents provide some basis for estimating the size distributions of material entering the Z-Plant exhaust duct system. In Mishima et al. (1968), size distributions are given for "production-run" fresh plutonium oxalate, partially oxidized oxalate, and plutonium tetrafluoride. The distributions of all these compounds had AMMDs in the 90- to 110- $\mu\text{m}$  range and standard deviations between 1.1 and 1.5; the distributions were approximately lognormal. Another document (Mishima et al. 1978) gives, for  $\text{PuO}_2$  used for fuel fabrication, a size distribution with an AMMD of about 25  $\mu\text{m}$ , a standard deviation of about 1.7, and noticeable deviations from lognormality. In experiments, a 1-m/s airstream was directed upward in annular flow around 1-g samples of these compounds. The aerosol removed by this airflow typically had size distributions that were similar to but finer than those of the samples; decreases in AMMD of about 30% were observed (Mishima et al. 1968).

Size distributions of about 20- $\mu\text{m}$  AMMD and 1.7 standard deviation (for oxide) and 70- $\mu\text{m}$  AMMD and 1.5 standard deviation (for the other compounds) may roughly represent the process material entering the Z-Plant ducts upstream of the HEPA filters. The material resulting from waste incineration (232-Z activity) might be represented by a size distribution for plutonium-containing ash from combustion of contaminated solid material. This aerosol had a mean diameter of 2.1- $\mu\text{m}$  AED and a standard deviation of 6.4, as measured by Mishima and Schwendiman (1973b). It is not clear what effect the 232-Z scrubbing system would have had on the ash size distribution, however.

The filters can be expected to have somewhat changed the size distribution of all aerosols, because they are slightly less efficient for the 0.3- to 1.0-AED range than for larger particle sizes (Tillery et al. 1984). However, unfiltered material (escaping during filter changeouts and failures) has probably also contributed to exhaust aerosol and deposition. Coagulation of the aerosol is another mechanism that could affect the size distribution of the material entering the exhaust system.

Both the deposition and adhesion of the exhaust aerosol are dependent on the size distribution. The fractions of aerosol in several size categories for process plutonium oxide, process non-oxide plutonium compounds, and plutonium-contaminated ash are given below.

<u>Particle AED Range (<math>\mu\text{m}</math>)</u>	<u>Plutonium Oxide</u>	<u>Plutonium Oxalate, Fluoride</u>	<u>Contaminated Ash</u>
< 0.3	0	0	0.15
0.3 - 1.0	0	0	0.20
1.0 - 10	0.096	0	0.46
10 - 70	0.90	0.51	0.17
70 - 100	0.008	0.31	0.011
100 - 1000	0.001	0.18	0.01

#### 4.5.2 Adhesion Mechanisms in Z-Plant Ducts

The reactivity and solubility of the exhaust aerosol also contribute to its adhesion to the duct wall. Experiments indicate that air blown upward in an annulus around small samples of damp plutonium oxalate, partially oxidized oxalate, and oxide and fluoride powder produced one or two orders of magnitude as much aerosol from the two types of oxalate as from the oxide or fluoride. The authors hypothesized that resuspension was aided by the evaporation of moisture from the oxalate into the very dry sweep air (Mishima et al. 1968). If this was the explanation, the mechanism would not hold for some Z-Plant duct airflow conditions; relative humidity can be over 50%, with saturation conditions possible in winter. On the other hand, particles might be released during dryer conditions, when evaporation could occur.

There are also mechanisms that could greatly increase the permanent particle adhesion resulting from high-humidity conditions: one of these is the dissolution of the soluble salts that are likely to be part of the aerosol. The salts could easily form a crust after drying (when the high-humidity conditions are removed), and the crust would hold other material in place. In addition,  $\text{PuF}_4$  is slightly hygroscopic. Other mechanisms that might increase particle retention are (1) the deagglomeration in moisture of large particles into much smaller ones that are harder to remove and (2) the possible increase of oxidation or corrosion of the surface in contact with moist particles (Whitfield 1979). Because of these mechanisms, it seems likely that almost all particles that have been in contact with the duct wall during periods of humidity have become fixed there, unless they were removed by forces other than those exerted by airflow.

The adhesion and resuspension behavior of plutonium compounds in ducts could be quantified by the appropriate experimental data. However, there is a shortage of applicable existing measurements of resuspension of plutonium compounds or other metal compounds under airflow conditions.

#### 4.5.3 Experiments Applicable to Z-Plant Resuspension

The following five experiments represent the most nearly applicable experiments that were found in the literature.

1. Resuspension factors were measured for dust contamination of hot cells and a plutonium handling facility. In the hot cell, contamination came from cutting irradiated fuel, and the ventilation rate was 50-air changes per hour. When decontamination work was not underway, the geometric mean of the measured resuspension factors was  $2.3E-8/cm$ . When decontamination was underway, resuspension was  $1.8E-6/cm$ . When less disturbing activities such as provision transfer or radiation survey were going on, the resuspension was an intermediate value. For resuspension of  $PuO_2$  powder, the resuspension factor was in the above range and the size distribution had an MMD of 6.4 to  $26 \mu m$  and a geometric standard deviation of 2.3 to 2.7 (Matsui et al. 1988). In these measurements it is unclear whether geometric or aerodynamic diameter is meant. (There is roughly a factor of 3 difference for plutonium dioxide.) The air velocity and the force applied to the particulate to resuspend it are not quantified. The nature of the surface from which resuspension occurred and the sampling system and duration are not described. The applicability of these data is low because of the lack of experimental definition, and the fact that duct airflow was not involved.
2. Metal and metal-oxide particulates were poured through a 100-mesh screen and so deposited on a horizontal, 302 stainless steel foil deposition surface in a 7.6-cm diameter, horizontal pipe. Airflows across the sample of greater than 20 m/s were used in this apparatus. Forty-nine experiments were performed for nine sets of conditions, all with relative humidity < 60%, with tungsten,  $Fe_2O_3$ , nickel, manganese, and  $SnO_2$  powders of sizes under  $10 \mu m$ . Resuspension rates were expressed as the fraction of deposited mass resuspended/time; each experiment was about 5-min long. For tests with low mass-loading per surface area, particles were resuspended continuously; for high-loading tests, resuspension was characterized by "layer-stripping," or bursts of particle removal. This was believed to correspond to the difference between adhesive and autohesive forces. Powder size had a large influence: larger tungsten powder was not resuspended by layer-stripping. The effect of particle density was unclear, perhaps because the particle-bed density rather than the intrinsic density should be considered. Results for  $10\text{-}\mu m$  manganese and  $10\text{-}\mu m$  tungsten powders were quite different, possibly because of material characteristics other than density. Resuspension rates ranged from about  $1E-04$  to  $1E-01$  fraction of material per second. The rates generally increased with increasing airflow velocity, with decreasing particle size, and with sample loading density (Wright and Pattison 1984). It was not clear whether aerodynamic or geometric diameters were stated. These data are of uncertain applicability. Although the experiment was well characterized and pertained to duct flow, it used a very short measurement period, and the materials tested were loosely packed and not similar to plutonium in density or chemical characteristics.
3. Uranium oxide powder ( $U_3O_8$ ) of less than  $50\text{-}\mu m$  diameter was loaded onto 2-m square concrete paving stones at a density of  $180 g/m^2$ . For powder in the  $0\text{-}4\text{-}\mu m$  size range, the average resuspension factor measured 0.3 m up at the downwind edge of the loaded area was  $2.0E-06 m^{-1}$ ; for the

0-12- $\mu\text{m}$  range,  $1.5\text{E-}07\text{ m}^{-1}$ ; and for the full 0-50- $\mu\text{m}$  range,  $9\text{E-}08\text{ m}^{-1}$ . These values were measured outdoors over several days, with occasional light rains and wind speeds less than 5 m/s. No relationship between the resuspension of the powder and the wind speed was noted. Similar values were obtained three weeks later after weathering (Stewart 1967). The sampling techniques, forces acting on the particles, and exact meteorological conditions during the experiments were not specified. Because of the outdoors nature of these experiments, the data obtained from them are not particularly applicable.

4. Plutonium oxide (AMAD about 15  $\mu\text{m}$ ) and nitrate powders in water suspension were dripped onto various surface coverings on a laboratory floor. The stresses applied included the ventilation air flow and various levels of human activity (walking on the powder). The duration of each test was not stated, but the sampling system is described in some detail. For plutonium oxide, the resuspension factor at "36 steps/min" activity was in the range  $2\text{E-}09$  to  $6\text{E-}09/\text{m}$  for paper, PVC, and waxed linoleum surfaces; for unwaxed linoleum, it was about  $2\text{E-}08/\text{m}$ . For plutonium nitrate, the resuspension factor for paper and waxed linoleum was  $1\text{E-}10$  to  $2\text{E-}10/\text{m}$  for "36 steps/min," and the resuspension factor for PVC was  $3\text{E-}10$  to  $2\text{E-}09/\text{m}$ . In the tests of paper floor covering, between 3 and 10% of the activity was in the form of oxide particles of less than 5  $\mu\text{m}$  attached to inert dust and fibers. The size distribution of particles in the air and on the floor appeared to be about the same; it had a geometric AMAD of about 10  $\mu\text{m}$  (Jones and Pond 1967). It would be difficult to apply these data to Z-Plant conditions because they do not pertain to duct flow, the resuspending forces are not quantified, and the surfaces do not resemble those in the ducts.
5. Aerosol particles of  $(\text{U,Pu})\text{O}_2$  with aerodynamic diameter of 7  $\mu\text{m}$  were put on substrates of aluminum, Plexiglas, chromium-plated steel, and brass. Centrifugal acceleration was applied over a 1-min period to determine the adhesive force. Particle retention was much greater (possibly 4 times as high) when all the data for several different successively higher accelerations were taken with a single deposit than when a fresh deposit was used for each acceleration test. The fresh-deposit procedure was therefore used throughout. The authors surmised that on successive accelerations the irregularly shaped particles that had not already been removed rearranged themselves for greater adhesion. There was no significant difference in adhesive forces measured in air at 40-50% relative humidity versus in nitrogen at 10% relative humidity. There was also not a significant difference between machined and polished surfaces or between aluminum, Plexiglas, and Cr-plated steel. Only the results with the brass substrate were significantly different (about 1/3 the adhesive force of the others). For the other three substrates, the force of adhesion for 50% removal was estimated to be  $8\text{E-}08\text{ N}$ , or 8% of the force estimated in the presence of capillary water (Pickering 1984). These data have considerable applicability for plutonium oxide in metal ducts under low-humidity conditions, but are limited to force of adhesion. They are therefore difficult to apply to determining resuspension rates or fractions.

Of these experiments, only one (the last) has any immediate relevance. It indicates that, where the capillary force is present in Z-Plant ducts, it will produce much more adhesion (and less resuspension) than can be expected in its absence. It is estimated that at all particle sizes below 100- $\mu\text{m}$  AED, Coulombic forces (based on equations in [Bowling 1985]) and weight forces should be negligible by comparison to molecular and double-layer forces (as measured by Pickering [1984]).

## 5.0 CONCLUSIONS AND RECOMMENDATIONS

The main points that have been found during this literature search are the following:

1. One of the weakest points in available data is the particle characterization. Deposition is largely dependent on the particle-size distribution. A "source-term" (exhaust system inlet) particle-size distribution would therefore be needed for any computer modeling of particle deposition. The measurements made in the stack do not necessarily indicate which of the upstream tributaries was the source of any particular portion of the size distribution, even though examination of individual particles gives clues as to their origin. In addition, the tendency of particles to be strongly fixed (encrusted) to the duct walls depends on the salt content of all the deposited particles, not just of the plutonium-containing particles. A 1971 sampling campaign did in fact find high salt content in aerosol samples taken from the end of the 236-Z line. Thus both the composition and the size distribution of aerosol are of importance. Particle-size measurements carried out during plant shutdown may not be of use; however, because deposition probably occurred primarily during production. Such measurements may be indicative of the resuspension that is occurring.
2. While deposition can be well characterized for modeling purposes, adhesion can be quantified only well enough to allow estimates of the relative importance of the different types of adhesive forces. There is no definitive way to convert adhesion forces into particle detachment rates. In fact, neither particle rebound nor detachment -- which together determine resuspension -- can be well quantified with current information. It follows that only upper-limit deposition estimates can be obtained. Resuspension tests conducted with simulated duct-deposit material would be needed to provide particle detachment data.
3. Adhesion of the particles is strongly affected by the relative humidity of the airflow and the wall temperature, which control the near-wall humidity. When the near-wall humidity exceeds 65%, capillary forces come into play; they are about 12 times as strong as the forces available to produce adhesion at a lower humidity. Thus, ducts exposed to outside air may accumulate particles during parts of the winter when condensation occurs. There is also some question as to whether there could be enough condensation to wash deposited particles into the low points in ducts. The conditions in outside ducts should be determined if possible.
4. Several of the aerosol samples taken in 1971 contained relatively small amounts of plutonium apparently bound to other particles, such as moist rust. In another (236-Z line), it seemed to be moist rust. This is strong evidence of resuspension and corrosion of the duct surface. Visual examination of the duct surface is needed to confirm this.

5. Estimates of deposition velocity show that, on the whole, deposition is most affected by vapor motion toward the walls (if condensation is occurring), by temperature gradients (for walls cooler than the gas), and by diffusion for particles of 1- $\mu\text{m}$  AED or smaller. Above that size and below 100- $\mu\text{m}$  AED, sedimentation and, in bends, centripetal acceleration are the most important deposition mechanisms for air velocities of about 20 ft/s. At velocities of about 50 ft/s, inertial deposition can also significantly increase the deposition of 7- to 70- $\mu\text{m}$  AED particles in ducts of 5-ft diameter or less. These results mean, in general, that most deposition will be found on the bottoms of ducts and possibly the outside radius of duct bends because of the prevalence of sedimentation over less directional forms of deposition.
6. The deposition velocity of particles of below 10- $\mu\text{m}$  AED is so low (less than 0.5 cm/s in straight ducts) that only a small fraction of these particles are likely to be deposited in the several-minute travel time from the final HEPA filters to the stack. It is also likely that some but not all particles larger than about 7- to 10- $\mu\text{m}$  AED rebound from surfaces, at the prevailing air velocity of about 20 ft/s. This may partly explain why sampling in the early 1970s found that aerosols from several parts of the Z-Plant exhaust system had median activity diameters of 3- to 10- $\mu\text{m}$  AED.

## 6.0 REFERENCES

- Balashazy, I., T. B. Martonen, and W. Hofmann. 1990. "Simultaneous Sedimentation and Impaction of Aerosols in Two-Dimensional Channel Bends." Aerosol Science and Technology 13:20-34.
- Beal, S. K. 1970. "Deposition of Particles in Turbulent Flow on Channel or Pipe Walls." Nuclear Science and Engineering 40:1-11.
- Bowling, R. A. 1985. "An Analysis of Particle Adhesion on Semiconductor Surfaces." Journal of the Electrochemical Society 132:2208-2214.
- Chan, M. K., M. Y. Ballinger, and P. C. Owczarski. 1989. User's Manual for FIRIN. PNL-4632, Pacific Northwest Laboratory, Richland, Washington.
- Davies, C. N. 1966. Aerosol Science, ed. C. N. Davies. Academic Press, New York.
- Forney, L. J., and L. A. Spielman. 1974. "Deposition of Coarse Aerosols from Turbulent Flow." Aerosol Science 5:257-271.
- Glissmeyer, J. A. 1992. Experimental Performance Evaluation of Two Stack Sampling Systems in a Plutonium Facility. PNL-8037, Pacific Northwest Laboratory, Richland, Washington.
- Jones, I. S., and S. F. Pond. 1967. "Some Experiments to Determine the Resuspension Factor of Plutonium from Various Surfaces." In Surface Contamination: Proceedings of a Symposium, ed. B. R. Fish, pp. 83-92. June 1964, Gatlinburg, Tennessee. Pergamon Press, New York.
- Liu, B. Y. H., and T. A. Ilori. 1974. "Aerosol Deposition in Turbulent Pipe Flow." Chemical Science and Technology 8:351-356.
- Matsui, H., Y. Ikezawa, Y. Izumi, H. Tomii, J. Onodera, Y. Anazawa, H. Yamamoto, and Y. Yoshida. 1988. "Dispersion and Resuspension Factors of Radioactive Dusts Derived from Air Monitoring Data in JAERI." In Proceedings of the Seventh International Congress of the International Radiation Protection Association. April 10, 1988, Sydney, Australia. Pergamon Press, Sydney, Australia.
- Mishima, J., L. C. Schwendiman, and C. A. Radasch. 1968. Plutonium Release Studies III. Release from Heated Plutonium Bearing Powders. BNWL-786, Pacific Northwest Laboratory, Richland, Washington.
- Mishima, J., and L. C. Schwendiman. 1971. Characterization of Radioactive Particles in the 234-5Z Building Ventilation Systems Interim Report. BNWL-B-105, Pacific Northwest Laboratory, Richland, Washington.
- Mishima, J., and L. C. Schwendiman. 1973a. Characterization of Radioactive Particles in the 234-5Z Building Gaseous Effluent. BNWL-B-309, Pacific Northwest Laboratory, Richland, Washington.

- Mishima, J., and L. C. Schwendiman. 1973b. Fractional Airborne Release of Uranium (Representing Plutonium) During the Burning of Contaminated Wastes. BNWL-1730, Pacific Northwest Laboratory, Richland, Washington.
- Mishima, J., L. C. Schwendiman, and J. E. Ayer. 1978. An Estimate of Airborne Release of Plutonium from the Babcock and Wilcox Plant as a Result of Severe Wind Hazard and Earthquake. PNL-2812, Pacific Northwest Laboratory, Richland, Washington.
- Ounis, H., and G. Ahmadi. 1990. "A Comparison of Brownian and Turbulent Diffusion." Aerosol Science and Technology 13:47-53.
- PFP Engineering Laboratory. 1989. Plutonium Holdup Downstream of Final HEPA Filtration. Technical Memo EDT-101762 to J. J. Roemer, Westinghouse Hanford Company, Richland, Washington.
- Pickering, S. 1984. "Adhesion of Aerosol Particles to Surfaces." In Proceedings of the First International Aerosol Conference. September 17-21, 1984, Minneapolis, Minnesota. Elsevier, New York.
- Postma, A. K. 1961. Studies in Micromeritics II. The Deposition of Particles in Circular Conduits Due to Thermal Gradients. HW-70791, Hanford Atomic Products Operation, General Electric Co., Richland, Washington.
- Ranade, M. B. 1987. "Adhesion and Removal of Fine Particles on Surfaces." Aerosol Science and Technology 7:161-176.
- Rogers, L. N., and J. Reed. 1984. "The Adhesion of Particles Undergoing an Elastic-Plastic Impact with a Surface." Journal of Physics D: Applied Physics 17:677-689.
- Schilling, A. E. 1989. Plutonium Finishing Plant (PFP) Remediation Project Management Plan. SD-CP-PMP-003, Rev. 0, Westinghouse Hanford Company, Richland, Washington.
- Schilling, A. E. 1990. Plutonium Finishing Plant (PFP) Final Safety Analysis Report (Draft). WHC-SD-CP-SAR-021, Westinghouse Hanford Company, Richland, Washington.
- Sehmel, G. A. 1968. Aerosol Deposition from Turbulent Airstreams in Vertical Conduits. BNWL-578, Pacific Northwest Laboratory, Richland, Washington.
- Stewart, K. 1967. "The Resuspension of Particulate Material from Surfaces." In Proceedings of the Surface Contamination Symposium, ed. B. R. Fish, pp. 63-74. June 1964, Gatlinburg, Tennessee. Pergamon Press, New York.
- Strom, L. 1988. "Airborne Particles in the Ventilation System of a BWR." In Proceedings of the 20th DOE/NRC Nuclear Air Cleaning Conference, pp. 814-823. August 22-25, 1988, Boston, Massachusetts. NUREG/CP-0098. Vol. 2., U.S. Nuclear Regulatory Commission, Washington, D.C.

Tillery, M. I., M. Gonzales, J. Elder, G. Royer, and H. J. Ettinger. 1984. "Measurements of the Penetration of High Efficiency Air Filters Using Plutonium Oxide Aerosols." In Proceedings of the First International Aerosol Conference. September 17-21, 1984, Minneapolis, Minnesota. Elsevier, New York.

Tsai, C. J., and D. Y. H. Pui. 1990. "Numerical Study of Particle Deposition in Bends of a Circular Cross-Section -- Laminar Flow Regime." Aerosol Science and Technology 12:813-831.

Vogt, E. C. 1982. Z Plant Plutonium Handling Operations Safety Analysis Report. RHO-CD-1244, Rockwell Hanford Operations, Richland, Washington.

Vogt, E. C., J. J. Roemer, and G. L. Jones. 1983. Plutonium Finishing Plant Safety Anaysis Report. SD-HS-SAR-007, Rev. 2, Rockwell Hanford Operations, Richland, Washington.

Whitfield, W. J. 1979. "Study of the Effects of Relative Humidity on Small Particle Adhesion to Surfaces, Surface Contamination Genesis, Detection, and Control." In Proceedings of Fourth International Symposium on Contamination Control, Vol. 1. September 10-14, 1978, Washington, DC. Plenum Press, New York.

Williams, R., and R. W. Nosker. 1985. "Dust." Chemtech 15:434-439.

Wright, A. L., and W. L. Pattison. 1984. "Results from Simulated Upper-Plenum Aerosol Transport and Aerosol Resuspension Experiments." In Proceedings of the CSNI Specialist Meeting on Nuclear Aerosols in Reactor Safety. September 4-6, 1984, Karlsruhe, Federal Republic of Germany. Kernforschungszentrum Karlsruhe GmbH, Karlsruhe, F. R. G.

Zimon, A. D. 1969. Adhesion of Dust and Powder. Plenum Press, New York.

DISTRIBUTION

No. of  
Copies

No of  
Copies

OFFSITE

12 DOE/Office of Scientific and  
Technical Information

ONSITE

2 DOE Richland Operations Office

J. E. Mecca R3-81  
D. W. Templeton R3-81

16 Westinghouse Hanford Company

R. E. Barker H5-71  
W. E. Davis H6-20  
J. D. Dick T4-20  
A. L. Ehlert T5-57  
G. A. Glover T4-20  
F. C. Han L5-07  
C. M. Kronvall T5-53  
D. J. McBride T5-54  
G. M. Stevens A4-79  
J. A. Teal H5-71  
E. C. Vogt T5-50  
G. A. Westsik (5) T5-53

17 Pacific Northwest Laboratory

M. Y. Ballinger P7-68  
J. G. Droppo K6-55  
J. A. Glissmeyer (5) K6-55  
S. J. Jette P7-68  
L. A. Mahoney (2) K7-15  
B. J. Tegner K6-86  
L. M. Thomas P8-44

Publishing Coordination K1-06  
Technical Report Files (5)

Routing

R. M. Ecker Sequim  
M. J. Graham K6-78  
P. M. Irving K6-98  
S. A. Rawson K6-81  
P. C. Hays/B. J. Tegner (last) K6-86